*Revised Manuscript
Click here to view linked References
https://doi.org/10.1016/j.conbuildmat.2020.118969
This is the Pre-Published Version.

Effects of Loading Mode on Mechanical Properties of High Strength Steel Q690 and Their Application in Coupon Test

Binhui Jiang[a,b], Zhihui Wang[b], Mengjie Wang[a], Michael C.H. Yam[b], Faxing Ding[a,*]

[a]*School of Civil Engineering, Central South University, 68 South Shaoshan Road, Changsha 410075, China*
[b]*Department of Building and Real Estate, The Hong Kong Polytechnic University, Hong Kong, China*

Abstract: The coupon test methods specified in the current specifications do not satisfactorily address the strain rate effect on mechanical properties of materials, which may cause some deviations in the results. Therefore, there is a demand for alternative loading modes of coupon test. In this paper, effects of loading mode on the mechanical properties of high strength steel (HSS) Q690 were tested, considering monotonic tensile coupon test, tensile coupon test with displacement-controlled holds, and tensile coupon test with strain-controlled holds. Parameters such as pre-strain, loading rate, hold times, and hold duration were considered. Results show that the yield strength, ultimate strength, and ultimate strain of steel Q690 were hardly affected by the stress relaxation induced by holds, while increase with the increase of loading rate. The largest difference of the ultimate strength induced by loading mode was 6.2 Mpa which is less than 1% of the ultimate strength of the material, and that of the ultimate strain was 5.8E-3. The stress drop during stress relaxation increases with the increase of pre-strain and strain rate. The normalized stress drop at the pre-strain of 0.04 could be 37.4% larger than that at the pre-strain of 0.01. The normalized stress drop of specimen with strain rate of 0.001 /s could be 27.7% larger than that with strain rate of 0.0001 /s. Tensile coupon test with two displacement-controlled holds is proposed to obtain the static mechanical properties of HSS Q690. Based on the test results, the values of parameters of the Cowper-Symonds model were calibrated to consider the effect of strain rate on the dynamic yield strength and ultimate strength, respectively, of steel Q690.

Keywords: High strength steel; material property; tensile coupon test; loading mode; stress relaxation; strain rate

1. Introduction

Steel is widely used in structural members due to its good mechanical properties, weldability, and adaptability to fast construction. With the development of material science, the application of high strength steel (HSS) such as steel Q690 to civil engineering structures has received attentions in the design and research community [1-4]. To conduct structural design or analysis, the mechanical properties such as elastic modulus, yield strength, ultimate strength and ultimate strain of the structural material need to be obtained. Research studies [5-9] have shown that metallic material is sensitive to the loading rate, indicating that the mechanical properties of metallic

*Corresponding author at: School of Civil Engineering, Central South University, Changsha 410075, China.
E-mail: dinfaxin@csu.edu.cn (F. Ding).

© 2020. This manuscript version is made available under the CC-BY-NC-ND 4.0 license https://creativecommons.org/licenses/by-nc-nd/4.0/

material will be different under different loading rates. During the service life of a structure, it may subject to static loads for most of the time, but sometimes may also be required to resist dynamic loads, such as seismic and wind loads. Hence, it is essential to obtain accurately both the static and dynamic mechanical properties of steel at different loading rates.

The mechanical properties of steel Q690 have been studied by several researchers. Compared with mild steel, steel Q690 has higher strength, higher yield ratio but smaller ultimate strain [10,11]. Huang et al. [12] and Wang et al. [13] studied the mechanical properties of steel Q690 at elevated temperatures, and found that the reduction factors of mechanical properties of steel Q690 at elevated temperatures are quite different from those of mild steel and those specified in the current mainstream structural design codes [14,15]. Li et al. [16] studied the post-fire mechanical properties of steel Q690 and found that the high-temperature treatment and cooling method have significant effects on the post-fire mechanical properties of steel Q690. Research studies of Kang et al. [17], Chen et al. [18] and Wang and Lui [19] showed that the mechanical properties of steel Q690 could keep unchanged if the highest experienced temperature is lower than a certain value, though the values of the temperature proposed by different researchers are different. It is noted that in the test of all the above studies, monotonic tensile test was used to obtain the mechanical properties of the steel Q690.

The testing procedure of tensile coupon test of metallic materials are available in specifications such as Australian Standard (AS) [20], European Code (BSI) [21], American Specification (ASTM) [22], and Chinese Standard [23]. These specifications specify a range of loading rate for monotonic tensile coupon test to represent a quasi-static loading condition. However, research of Huang and Young [24] indicated that the effect of loading rate on mechanical properties cannot be fully addressed even though the specified loading rate in the specifications is adopted. That is because the enhancement effect of strain rate on the strength of steel is notable even adopting a small loading rate which satisfies the requirement of the specifications [25]. Hence, to accurately obtain the static mechanical properties of steel material, alternative loading modes are required except for monotonic tensile test.

The dynamic strength of metallic material was assumed to be consist of two parts, namely, the static strength and an enhancement part due to strain rate effect [26]. Krempl and Khan [27] suggested that the stress enhancement due to loading rate could be eliminated by holding the coupon for a long time during the process of tensile coupon test, and thus to obtain the static strength. Stress drop will occur during the holding process due to stress relaxation [28], and the enhancement part due to strain rate effect is believed to be relaxed by stress relaxation [29,30]. The stress relaxation test was initially adopted in coupon test by Hart and Solomon [31] to obtaining the performance of polycrystalline aluminium considering a wide range of strain rates while the developed strain is small. Research of Haut and Lion [25] indicated that the equilibrium states of a viscoplastic material may be identified either by stress relaxation or creep, while stress relaxation was more recommended because it costs less time. Stress relaxation has been adopted by researchers [32,33] in tensile coupon tests to obtain the static strength. Huang and Young [24] proposed a detailed procedure of tensile coupon test to obtain the static yield strength, ultimate strength, and static stress versus strain curve by adopting two holds in the process of tensile coupon test, based on their tests on cold formed steel and aluminium alloy.

On the other hand, experimental studies of researchers have shown that loading mode, such as tensile coupon test with holds, may alter the strength and ductility of metallic materials. Test of Varma et al. [34] showed that stress relaxation could improve the ductility of stainless steel SS 316L, and similar effect was found on titanium alloys by Eipert et al [35]. Research of Hannula et al. [36] showed that the duration of stress relaxation would affect the mechanical behaviour of type 316 stainless steel. Hariharan et al. [37] found that stress relaxation could improve the ductility of low carbon steel, dual phase (DP) steel, and transformation induced plasticity (TRIP) steel, and this improvement was different for different kinds of material. Xu et al. [38] showed that comparing with monotonic tension test, cyclic loading and unloading test significantly increased both the ultimate strength and ultimate strain of TRIP steel. Li et al. [39] found that stress relaxation due to holds during tensile coupon test could enhance the ultimate strength and ultimate strain of 304 stainless steel, and this enhancement was notably affected by the strain value at which the specimen was held. This strain value was referred to as pre-strain in the current study. Therefore, it is important to ensure that the intrinsic mechanical properties of structural steel used in structural design are not altered by the adopted loading mode of the tension coupons. However, the effect stress relaxation on the mechanical properties of steel Q690 has not been extensively investigated.

Based on the above, the object of the current study is focused on experimentally examining the effects of loading mode on mechanical properties of steel Q690 and proposing a suitable loading mode to obtain the static mechanical properties of this material. Three loading modes were considered, namely, monotonic tensile coupon test, tensile coupon test with displacement-controlled holds, and tensile coupon test with strain-controlled holds. The stress drop due to stress relaxation and the stress jump of post stress relaxation were also investigated by considering the effects of pre-strain, loading rate, hold times, and hold duration. Based on the test results, the parameters in the Cowper-Symonds (C-S) mode [26] were calibrated to consider the strain rate effect on the yield strength and ultimate strength of steel Q690, respectively. Finally, suggestions on procedures of conducting coupon test to obtain the static mechanical properties of HSS Q690 were proposed.

2. Experimental investigation

2.1 Specimens details

Tensile coupon tests were conducted on 29 flat specimens of HSS Q690. All the specimens were extracted from one single big steel plate with a thickness of 6 mm, and the length direction of the specimens was along the rolling direction of the steel plate. The delivery state of the steel is quenched, and the chemical compositions of it are shown in Table 1. The designed dimensions of the specimens are illustrated in Fig. 1, which conform to the American Specification ASTM E8/E8M-16a [22]. Fifteen series of tensile coupon tests were designed as listed in Table 2, including 3 series of monotonic tensile test, 3 series of tensile test with displacement-controlled holds, and 9 series of tensile test with strain-controlled holds. Both kinds of holds were achieved by controlling the displacement of the cross head of the test machine. For the displacement-controlled hold, the cross head of the test machine was firmly restrained, while for the strain-controlled hold the displacement of the cross head was controlled so that the strain of the coupon remains constant during the hold. As can be seen from Table 2, three different strain rates of 0.0001 s^{-1} 0.001 s^{-1} and 0.05 s^{-1} were considered to study the effect of strain rate on mechanical properties with or without holds. Huang and Young [24] suggested that the static stress-strain curve of steel could be obtained by conducting two holds during the tensile coupon test, one near the yield stress and the other near the ultimate strength. Hence, the current study considers two pre-strains, the strains at which the specimen was held, of 0.01 and 0.04, which are near the yield strain and ultimate strain of steel Q690, respectively. Besides, two values of pause time for the holds, 90 s and 300 s, were considered.

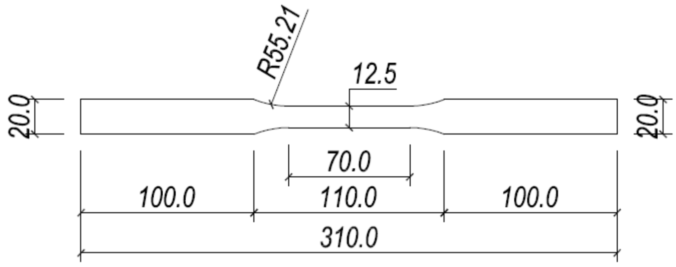

Fig. 1 Dimensions of the tested coupons (dimensions in mm)

As listed in Table 2, each series was labelled to show the information of the loading rate, hold control method, per-strain, and hold duration. The first character “S” represents strain rate, and the second number represents the value of strain rate. “S1”, “S2”, and “S3” represent the strain rates of 0.0001/s, 0.001/s, and 0.005/s, respectively. The two characters right after the first hyphen represent the control method of holds. “MO” represents monotonic tensile test without any holds, while “DH” and “SH” represent tensile test with displacement-controlled holds and strain-controlled holds, respectively. The number right after these two characters represents the number of hold. For the series with holds, the character "T" right after the second hyphen represents the pause time of each hold. "T1" and "T2" represent the pause time of 90 s and 300 s, respectively, for each hold. For example, the series labelled S1-DH2-T2 shows the coupon test was conducted with a strain rate of 0.0001/s, two displacement-controlled holds (at strain of 0.01 and 0.04, respectively), and the pause time of each hold was 300 s. Two coupon tests were conducted for the vast majority of the series.

Table 1 Chemical compositions of the studied HSS Q690 (in wt%)

C	Si	Mn	P	S	Nb	Ti
0.140	0.280	1.39	0.014	0.001	0.027	0.014
Cr	Mo	B	Ceq	Ni	N	Cu
0.26	0.15	0.0014	0.45	0.02	0.0029	0.01

Table 2 Summary of the test series

Series	Strain rate (s^{-1})	Loading mode	Pre-strain	Pause time (s)
S1-MO	0.0001	MO	--	--
S2-MO	0.001	MO	--	--
S3-MO	0.005	MO	--	--
S1-DH1-T2	0.0001	DH	0.04	300
S1-DH2-T2	0.0001	DH	0.01, 0.04	300
S2-DH2-T2	0.001	DH	0.01, 0.04	300
S1-SH1-T1	0.0001	SH	0.04	90
S1-SH1-T2	0.0001	SH	0.04	300
S1-SH2-T1	0.0001	SH	0.01, 0.04	90
S2-SH1-T1	0.001	SH	0.04	90
S2-SH1-T2	0.001	SH	0.04	300
S2-SH2-T1	0.001	SH	0.01, 0.04	90
S3-SH1-T1	0.005	SH	0.04	90
S3-SH1-T2	0.005	SH	0.04	300
S3-SH2-T1	0.005	SH	0.01, 0.04	90

Note: MO, DH and SH represent monotonic tensile test, tensile test with displacement-controlled hold, and tensile test with strain-controlled hold, respectively.

2.2 Test set-up

The Instron 8803 test machine with a load capacity of 500 kN was used to conduct the tensile coupon tests, as shown in Fig. 2. As can be seen from Fig. 2, tensile load was applied to the coupon specimen through the grips at both ends of it. The value of the applied load was monitored by a built-in load cell of the machine. An extensometer with a gauge length of 50 mm was adopted to measure the nominal strain of the test coupon.

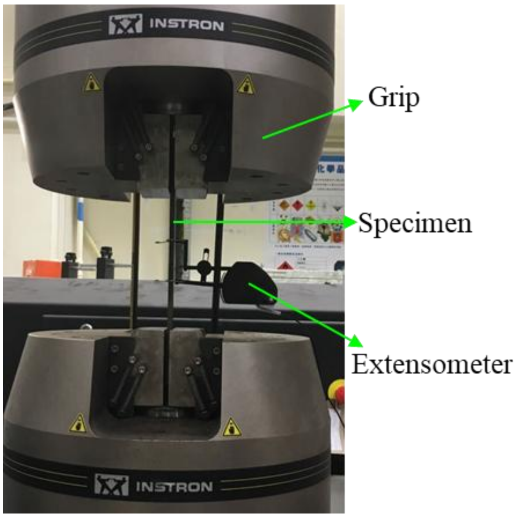

Fig. 2 Test set-up

2.3 Test procedures

During the test, the position of the upper grip was fixed while the lower grip moved downward to apply tensile load to the coupon specimens, as shown in Fig. 2. The movement of the lower grip was driven by displacement control, according to the targeted strain rate of the specimen. For each specimen, a constant strain rate was adopted during the whole loading process. Three strain rates were considered for the monotonic tensile tests to investigate the effect of strain rate on mechanical properties. For the coupon tests with holds, the movement of the lower grip will be held for a designed period of time at certain strains. For the displacement-controlled hold, the grip was firmly held. During this hold, the reading of the extensometer will increase slightly due to stress relaxation. For the strain-controlled hold, the grip was held in the way to ensure the reading of the extensometer remains constant during the hold, which was automatically controlled by the machine once the settings were completed by the test operator. For the tests with one hold, the pre-strain, at which the hold started, was 0.04, while the pre-strains for the tests with two holds were 0.01 and 0.04, respectively. The pause time for all the tests with displacement-controlled holds was 300 s while two lengths of pause time were considered for the tests with strain-controlled holds, namely 300 s and 90 s, respectively.

3. Test results and discussion

3.1 Dynamic properties

Each specimen of the current study was conducted at a specific loading rate. As already explained, even though the loading rate conforms to the specifications, the effect of loading rate on mechanical properties cannot be fully addressed. Hence, the mechanical properties obtained from the stress-strain curves according to the specifications were dynamic mechanical properties at the specific loading rate. The representative strain-stress curves of the three series of monotonic tensile tests are shown in Fig. 3, which reflect the effect of strain rate on the material properties. The detailed mechanical properties of the monotonic tensile tests are listed in Table 3. As can be seen from Fig. 3 and Table 3, the strain rate has little effect on the elastic modulus of the material, while notable effects on the yield strength and ultimate strength. Fig. 4 shows the effect of strain rate on the material strength and ultimate strain of the tested steel material. It can be seen that both the yield strength and ultimate strength increase with the increase of strain rate. This phenomenon confirms the concern that even adopting the strain rate which matches the requirement of the current mainstream tensile test standards, the notable enhancement of strength due to the effect of strain rate still exists. It is also worth noting that the enhancement trend of ultimate strength due to strain rate is similar with that of yield strength. Besides, as can be seen from Fig. 3(b) and Table 3, the ultimate strain also increases with the increase of strain rate.

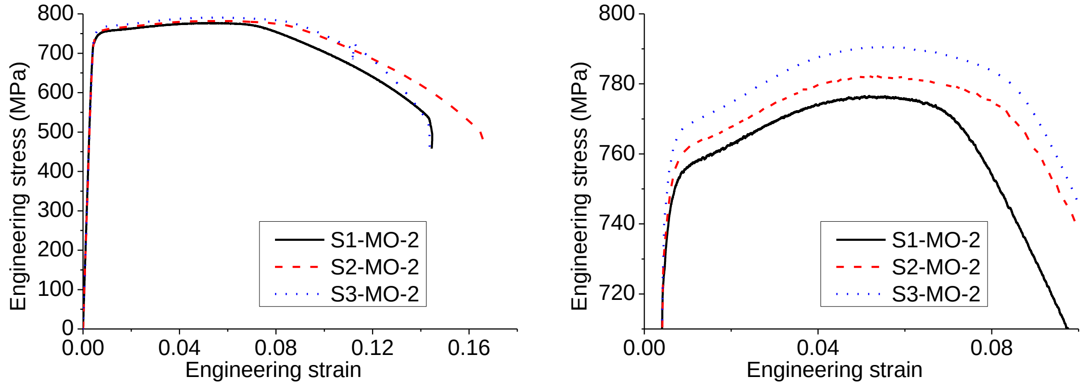

(a) Whole strain range (b) Partial strain range

Fig. 3 Strain-stress curves of monotonic tensile tests

Table 3 Material properties obtained from monotonic tensile tests

Specimen	E (GPa)	$\sigma_{0.2}$ (MPa)	σ_u (MPa)	ε_u (E-2)
S1-MO-1	189.5	743.3	776.9	5.24
S1-MO-2	192.6	743.1	776.5	5.18
Mean	**191.1**	**743.2**	**776.7**	**5.21**
S2-MO-1	189.9	754.2	786.8	5.13
S2-MO-2	188.8	748.6	782.6	5.56
Mean	**189.3**	**751.4**	**784.7**	**5.34**
S3-MO-1	189.1	773.6	796.1	5.54
S3-MO-2	187.3	757.4	790.5	5.69
Mean	**188.2**	**765.5**	**793.3**	**5.61**

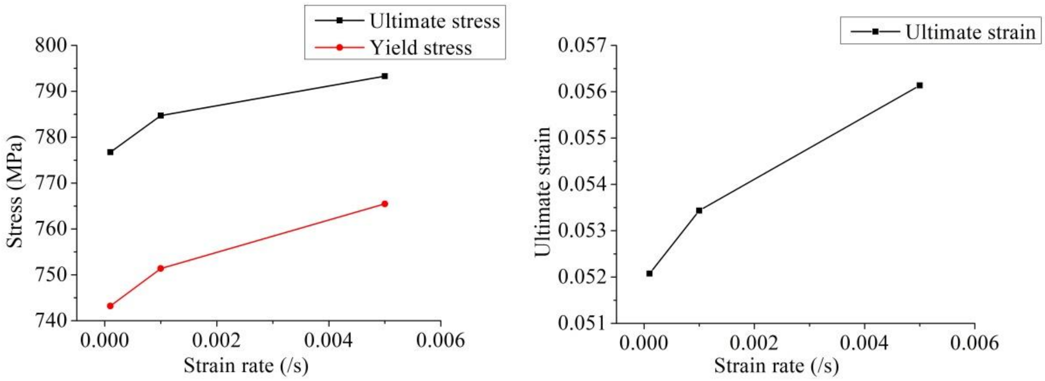

(a) Yield and ultimate stress (b) Ultimate strain

Fig. 4 Effects of strain rate of monotonic tensile test on mechanical properties

Table 4 Material properties obtained from tensile tests with displacement-controlled holds

Specimen	E (MPa)	$\sigma_{0.2}$ (MPa)	σ_u (MPa)	ε_u (E-2)
S1-DH1-T2-1	193.0	739.7	773.7	5.23
S1-DH1-T2-2	190.7	747.1	780.9	5.31
Mean	**191.9**	**743.4**	**777.3**	**5.28**
S1-DH2-T2-1	201.8	743.6	777.5	5.07
S1-DH2-T2-2	192.7	744.9	778.1	5.36
Mean	**197.3**	**744.3**	**777.8**	**5.22**
S2-DH2-T2-1	192.6	757.5	787.8	5.84
S2-DH2-T2-2	199.8	752.1	787.2	5.36
S2-DH2-T2-3	193.7	752.7	787.2	5.03
S2-DH2-T2-4	193.6	753.5	--	--
Mean	**194.9**	**753.9**	**787.4**	**5.41**

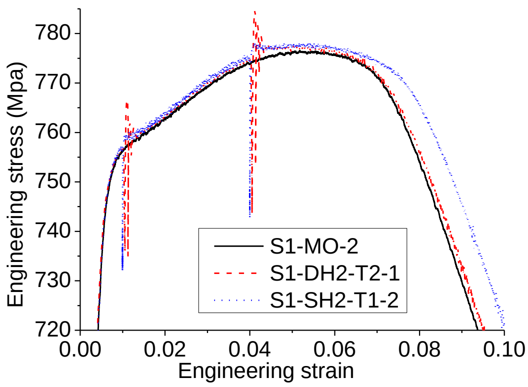

Fig. 5 Comparison of stress-strain curves between monotonic tensile test and tests with holds

Detailed dynamic mechanical properties of specimens obtained from tensile tests with displacement-controlled holds are listed in Table 4, and those obtained from tensile test with strain-controlled hold are listed in Table 5. Fig. 5 presents a comparison of strain-stress curves of three specimens obtained from tensile tests with the same strain rate of 0.0001 /s but different loading modes, namely, monotonic tensile test (S1-MO-2), tensile test with displacement-controlled holds (S1-DH2-T2-1), and tensile test with strain-controlled holds (S1-SH2-T1-2). It can be seen that in general both the displacement-controlled holds and the strain-controlled holds have little effect on the stress-strain curve of the tested specimens until the stress reached the ultimate strength, except for the localized stress drop due to stress relaxation and reloading when being held. Photos of the tests with strain rate of 0.0001 /s of the above three loading modes, including these presented in Fig. 5, are shown in Fig. 6. It should be noted that for the convenience of description, the labels of the specimens adopted in the manuscript are different with those marked on the specimens. All the specimens in Fig. 6 were fractured, except for S1-DH2-T2-2, the test of which was stopped after it was necked. It can be seen from Fig. 6 that the difference of elongations after fracture of the specimens is small.

Table 5 Material properties obtained from tensile tests with strain-controlled holds

Specimen	E (MPa)	$\sigma_{0.2}$ (MPa)	σ_u (MPa)	ε_u (E-2)
S1-SH1-T1-1	192.8	747.1	782.3	5.38
S1-SH1-T1-2	192.2	746.0	779.7	5.54
Mean	**192.5**	**746.5**	**781.0**	**5.46**
S1-SH2-T1-1	193.5	747.8	782.0	5.43
S1-SH2-T1-2	190.3	743.9	778.2	5.16
Mean	**191.9**	**745.9**	**780.1**	**5.29**
S1-SH1-T2-1	194.6	742.2	775.0	5.16
S1-SH1-T2-2	192.5	741.1	774.6	5.32
Mean	**193.6**	**741.7**	**774.8**	**5.24**
S3-SH1-T1-1	189.4	760.8	795.0	5.19
S3-SH1-T1-2	189.2	754.2	788.6	5.17
Mean	**189.3**	**757.5**	**791.8**	**5.18**
S3-SH2-T1-1	191.1	755.2	789.2	4.93
S3-SH2-T1-2	190.9	752.8	787.2	5.12
Mean	**191.0**	**754.0**	**788.2**	**5.03**
S3-SH1-T2-1	191.9	755.3	789.1	5.44
S3-SH1-T2-2	192.2	756.9	790.3	5.12
Mean	**192.1**	**756.1**	**789.7**	**5.28**
S2-SH1-T1-1	190.6	751.9	782.8	5.49
S2-SH1-T2-1	185.8	748.6	783.4	5.26
S2-SH2-T1-1	186.6	749.1	782.1	5.23

Fig. 7 shows the dynamic ultimate strength and ultimate strain of all the 15 series tests. It can be seen from Fig. 7 (a) that for all the three loading modes, the dynamic ultimate strength increases with the increase of the strain rate. On the other hand, the loading modes have little effect on the dynamic ultimate strength for all the considered strain rates, with the largest difference induced by loading mode being 6.2 MPa which is less than 1% of the ultimate strength. As shown in Fig. 7(b), for the specimens of monotonic tensile test and tensile test with displacement-controlled holds, the ultimate strain increases with the increase of strain rate, while for the specimens of tensile test with strain-controlled holds the effect of strain rate shows no obvious trend. The largest differences of ultimate strain induced by loading modes were 2.5E-3, 2.6E-3, and 5.8E-3 for the strain rate of 0.0001 /s, 0.001 /s, and 0.005 /s, respectively. Hence, in general, the effects of the considered loading modes on both the ultimate stress and the ultimate strain of HSS Q690 are small, especially for the specimens with low strain rate. This indicates that tensile test with holds do not alter the dynamic properties of HSS Q690.

Fig. 6 Photos of specimens with strain rate of 0.001 /s of monotonic tensile test and tests with holds after the coupon tests

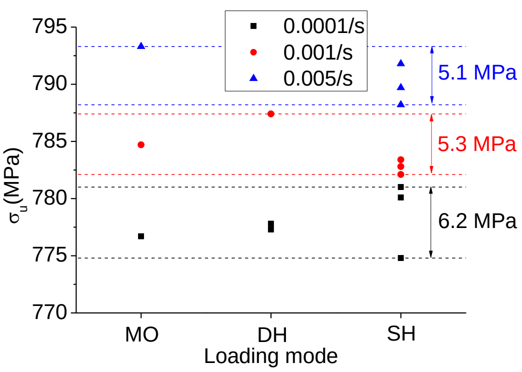

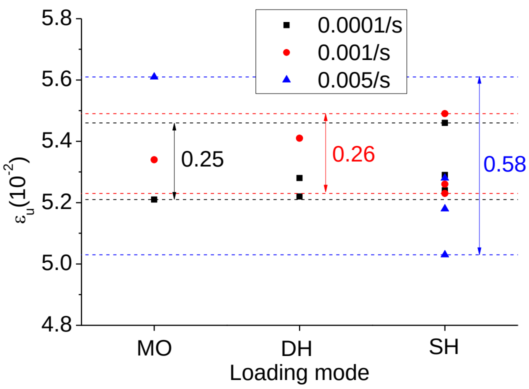

(a) Ultimate strength (b) Ultimate strain

Fig. 7 Effects of stress relaxation on mechanical properties of the tested steel

3.2 Stress drop

Typical strain-stress curves near the pre-strain of the specimens of tensile test with strain-controlled holds are presented in Fig. 8. As can be seen from the figure, for the tensile tests with strain-controlled holds, the strain decreased slightly when the specimen was held. This may be due to the fact that for this loading mode, the cross head of the machine withdrew a little when the specimen was held, which indicates that the stress drop at the holds is a result of the combination of stress relaxation and unloading. It is also noted that the lowest stresses at the stress drop of different strain rates are different, and the lowest stress decreased with the increase of strain rate. This phenomenon indicates that the obtained static strengths according to this loading mode are not concordant for specimens with different loading rates. Therefore, strain-controlled hold is not a suitable method to obtain the static mechanical properties of the material.

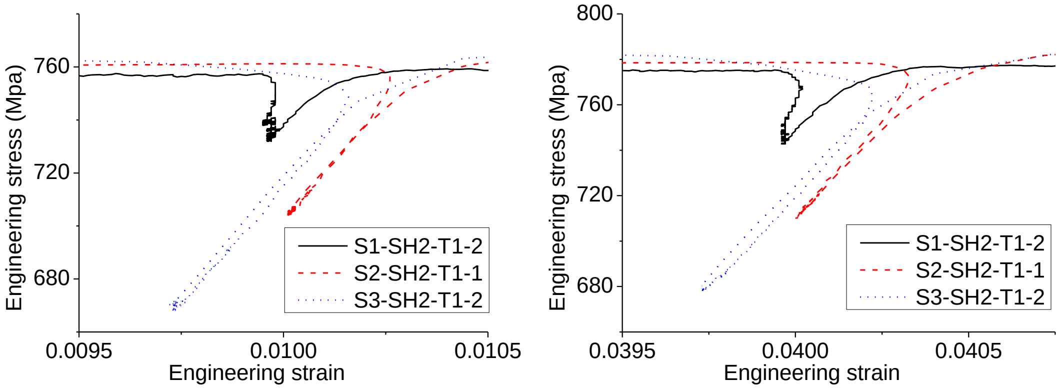

(a) Hold at strain of 0.01 (b) Hold at strain of 0.04

Fig. 8 Comparison of stress drop due to strain-controlled hold

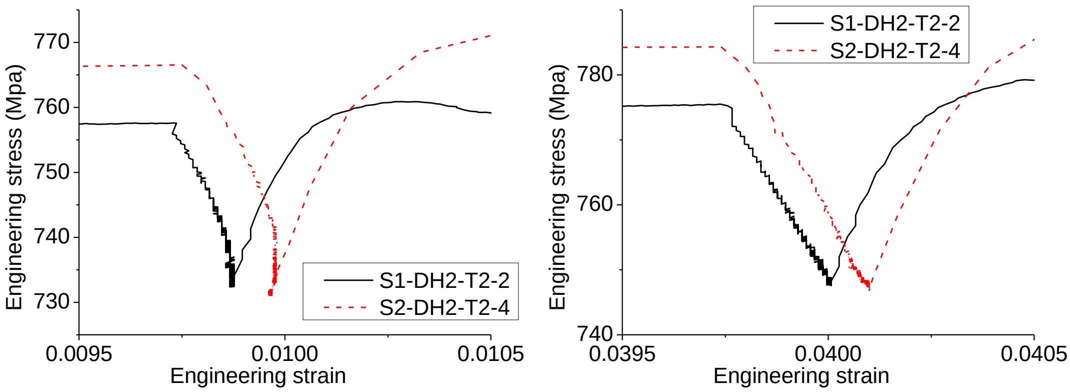

(a) Hold at strain of 0.01 (b) Hold at strain of 0.04

Fig. 9 Comparison of stress drop due to displacement-controlled hold

Fig. 9 shows two typical strain-stress curves near the pre-strain of the specimens of tensile test with displacement-controlled holds. As can be seen from Fig. 9, the strain was increased slightly while the stress was decreased notably. When the displacement of the cross head of the machine was held, the strain of the specimen continued to increase slightly due to stress relaxation. It is noted that the stresses prior to the hold of the specimens with different strain rates were different due to the effect of strain rate, while the lowest stress at the stress drops of all the specimens were almost the same. This lowest stress at the stress drop represents the static stress value at this strain. Fig. 10 shows the effects of the pre-strain, strain rate, and pre-hold on the stress drop of stress relaxation. The stress in Fig. 10 was normalized by the stress value at the initial point of the stress drop. As can be seen from Fig. 10(a), for a relaxation duration of 300s of the specimen labelled S1-DH2-T2-1, the normalized stress drops at the pre-strains of 0.01 and 0.04 were 2.73E-2, and 3.75E-2, respectively. Hence, the normalized stress drop at the pre-strain of 0.04 was 37.4% larger than that at the pre-strain of 0.01. Fig. 10(b) illustrates that the normalized stress drop of the specimen with strain rate of 0.001 /s was 4.79E-3, while that of the specimen with strain rate of 0.0001 /s was 3.75E-3. Hence, the normalized stress drop of specimen with strain rate of 0.001 /s was 27.7% larger than that with strain rate of 0.0001 /s. Fig. 10(c) compares the stress drop at the pre-strain of 0.04 between specimen S1-DH1-T2-1 and S1-DH2-T2-1. The specimen S1-DH2-T2-1 was held for 300 s at pre-strain of 0.01 prior to the hold at pre-strain of 0.04, while there was no pre-hold for S1-DH1-T2-1. It is shown in Fig. 10 (c) that the stress drops of both specimens are almost the same, illustrating that pre-hold has negligible effect on the dress drop of stress relaxation.

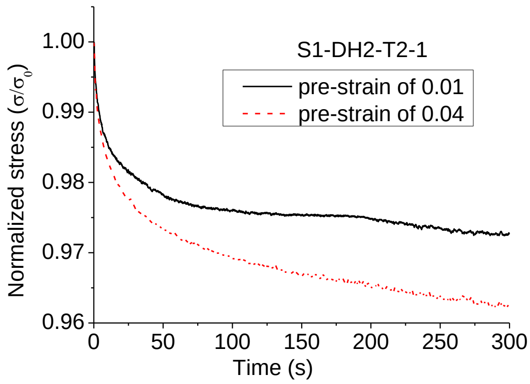

(a) Effect of pre-strain

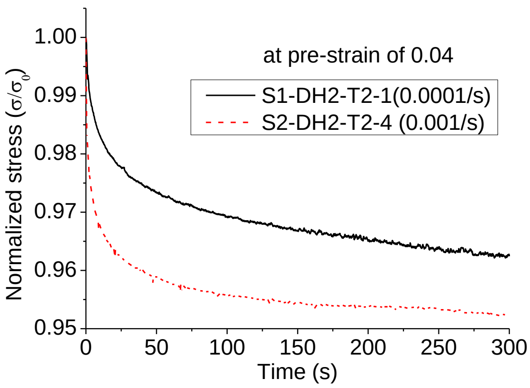

(b) Effect of strain rate

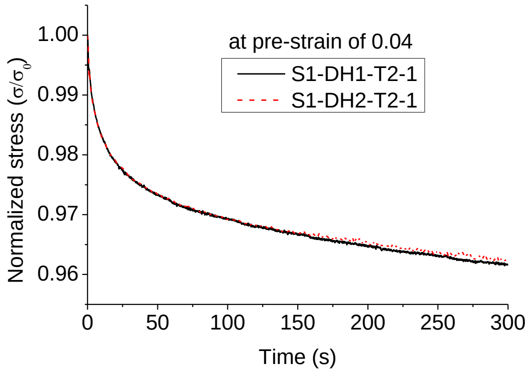

(c) Effect of pre-hold

Fig. 10 Effects of pre-strain, strain rate and pre-hold on the stress drop of hold

3.3 Stress jump of post hold

Fig. 11 shows the stress-strain curve of a representative specimen with displacement controlled holds and re-loading after the hold. The hold began at point *a* and ended at point *b*, followed by reloading. It is noted that in the process of reloading, the stress was increased first, then declined after reaching a localized peak stress point (point *c*). The stress continued to decrease until reaching point *d* where the stress started to increase again. Hence, there is a stress jump between point *a* and point *c*, which could be represented as σ_c-σ_a. Besides, it can be seen that the stress-strain curve between points *a* and *d* was disturbed by the hold, compared with normally adopted monotonic tensile coupon test. For monotonic tensile coupon test, the stress should continue to raise from point *a* to point *d*. The strain difference between point *d* and *a*, namely ε - is defined as the affected strain range in the current work. It is of importance to note that if the intrinsic ultimate strength point of the material locates in the strain range between ε_a and ε_d, the stress after point *c* will not return to increase any more, making it difficult to identify the ultimate strength point, as illustrated in Fig. 12. Therefore, in coupon test the pre-strain of hold should be chosen properly so that the characteristic points such as the yield strength point and the ultimate strength point do not locate in the affected strain range.

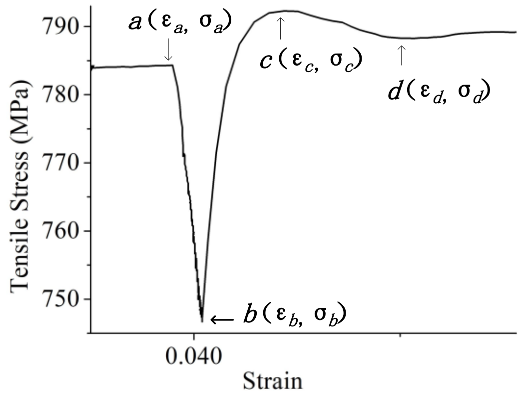

Fig. 11 Stress-strain curves of displacement-controlled hold

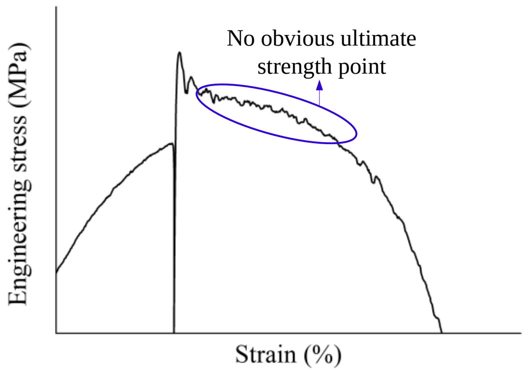

Fig. 12 Stress jump makes it difficult to identify the ultimate strength point

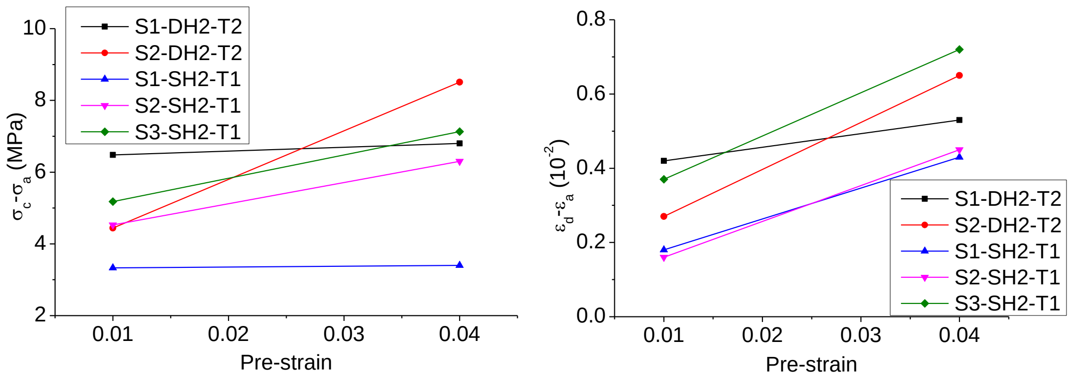

(a) Stress jump (b) Affected strain range

Fig. 13 Effects of the value of pre-strain

Table 6 Material properties obtained from tensile tests with displacement-controlled holds

Pre-strain Specimen	0.01 -*σ* (MPa)	0.01 -*ε* (E-2)	0.04 -*σ* (MPa)	0.04 -*ε* (E-2)
S1-DH1-T2-1			3.93	0.63
S1-DH1-T2-2			5.38	0.68
Mean			**4.65**	**0.65**
S1-DH2-T2-1	9.67	0.31	9.83	0.51
S1-DH2-T2-2	3.29	0.53	3.77	0.55
Mean	**6.48**	**0.42**	**6.80**	**0.53**
S2-DH2-T2-1	1.68	0.26	9.67	0.32
S2-DH2-T2-2	5.04	0.36	7.41	0.99
S2-DH2-T2-3	5.42	0.24	9.01	0.97
S2-DH2-T2-3	5.62	0.23	7.96	0.29
Mean	**4.44**	**0.27**	**8.51**	**0.65**

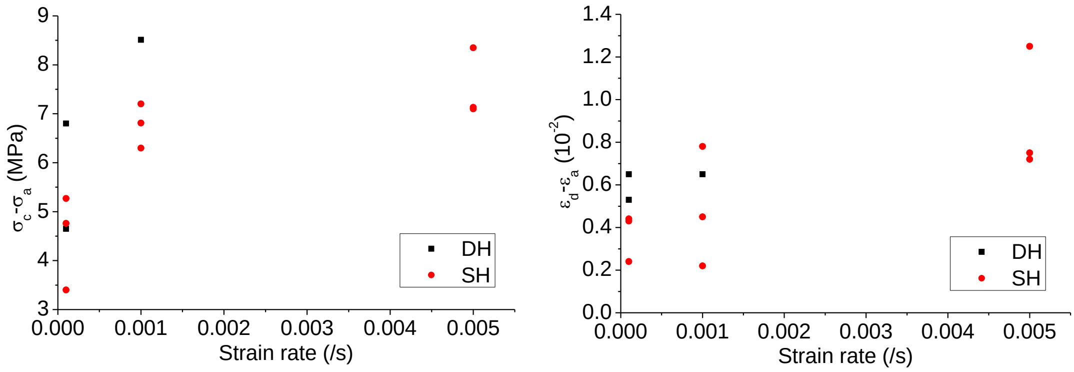

(a) Stress jump (b) Affected strain range

Fig. 14 Effects of strain rate

The stress jump and the affected strain range of all the specimens with displacement-controlled holds are listed in Table 6, and those of the specimens with strain-controlled holds are listed in Table 7. Fig. 13 shows the effect of the pre-strain on the stress jump and the affected strain range. It can be seen that both the stress jump and the affected strain range were increased with the increase of the value of pre-strain. Fig. 14 illustrated the effect of strain rate on the stress jump and the affected strain range for the hold at pre-strain of 0.04. As can be seen from Fig. 14, in general, both the stress jump and the affected strain range were increased with the increase of strain rate. Besides, among all the specimens, the largest affected strain ranges for specimens with strain rates of 0.0001 /s, 0.001 /s and 0.005 /s were 0.65E-2, 0.78E-2, and 1.25E-2, respectively. Fig. 15 shows the effect of pause time of the hold on the stress jump and the affected strain range of the test with strain-displacement holds for the hold at pre-strain of 0.04. It can be seen from Fig. 15 that the trends of effect of pause time on the stress jump and the affected strain range are not obvious.

Table 7 Stress jump and affected strain range of tensile tests with strain-controlled holds

Pre-strain Specimen	0.01 -σ (MPa)	0.01 -ε (E-2)	0.04 -σ (MPa)	0.04 -ε (E-2)
S1-SH1-T1-1			5.42	0.22
S1-SH1-T1-2			4.10	0.25
Mean			**4.76**	**0.24**
S1-SH2-T1-1	4.58	0.21	4.73	0.46
S1-SH2-T1-2	2.09	0.15	2.08	0.39
Mean	**3.33**	**0.18**	**3.40**	**0.43**
S1-SH1-T2-1			6.52	0.64
S1-SH1-T2-2			4.02	0.24
Mean			**5.27**	**0.44**
S3-SH1-T1-1			7.29	0.92
S3-SH1-T1-2			6.90	0.58
Mean			**7.10**	**0.75**
S3-SH2-T1-1	5.06	0.35	7.09	0.76
S3-SH2-T1-2	5.30	0.39	7.16	0.67
Mean	**5.18**	**0.37**	**7.13**	**0.72**
S3-SH1-T2-1			8.23	1.25
S3-SH1-T2-2			8.47	--
Mean			**8.35**	**1.25**
S2-SH1-T1-1			7.20	0.22
S2-SH1-T2-1			6.81	0.78
S2-SH2-T1-1	4.53	0.16	6.30	0.45

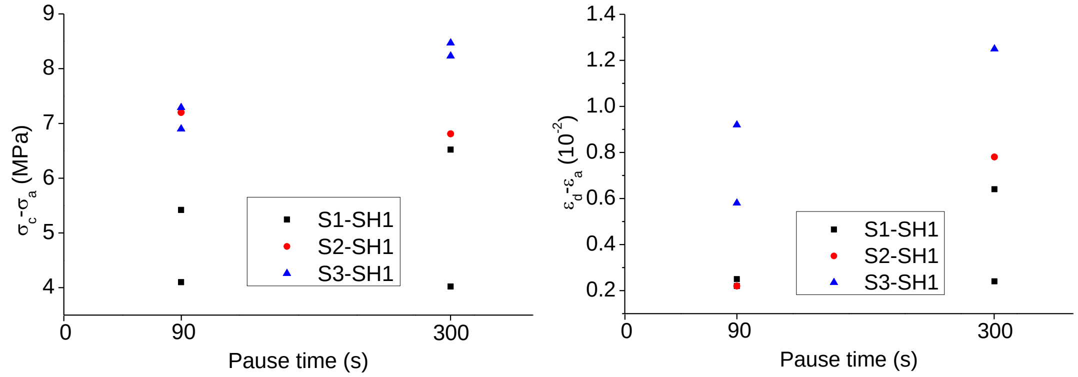

(a) Stress jump (b) Affected strain range

Fig. 15 Effects of pause time of holding

3.4 Static mechanical properties

The static mechanical properties of the tested steel material could be obtained from the results of the tensile coupon test with displacement-controlled holds, as listed in Table 8. The static yield strength is determined by subtracting the stress drop at the nearby hold from the dynamic yield strength. Similar procedure is adopted for determining the static ultimate strength. It can be seen from Table 8 that for tensile test with displacement-controlled holds the static strength and ultimate strength obtained from specimens with different strain rates were consistent, although the dynamic strengths were different as already presented in Section 3.1.

Table 8 Static material strengths obtained from tensile tests with displacement-controlled holds

Specimen	(MPa)	(MPa)
S1-DH1-T2-1	--	744.1
S1-DH1-T2-2	--	753.2
Mean	**--**	**748.7**
S1-DH2-T2-1	723.3	748.5
S1-DH2-T2-2	720.5	750.4
Mean	**721.9**	**749.5**
S2-DH2-T2-1	727.8	752.3
S2-DH2-T2-2	722.2	750.2
S2-DH2-T2-3	716.7	748.4
S2-DH2-T2-4	717.5	--
Mean	**721.0**	**750.3**

4. Evaluation of strain rate effect equations

There are several models to consider the effect of strain rate on the dynamic strength of metal material of which the Cowper-Symonds (C-S) model [26] is widely used for steel. For different grades of steel, the value of parameters in the strain rate effect models may be different. This section calibrates the value of the parameters in the C-S model using the test results of the steel Q690. According to the C-S model, the dynamic increase factor (DIF), which is the ratio of dynamic strength and static strength, is a function of the strain rate, as illustrated in Eq. 1:

(1)

where σ_{dy} and σ_{sy} are the dynamic yield strength and static yield strength, respectively; $\dot{\varepsilon}$ is the strain rate; C and P are material parameters. The values of C and P could be obtained from curve fitting of test results. Fig. 16 shows the curve fitting of the DIF of the yield strength and ultimate strength of the current tests. The values of C and P are 1.203E8 and 8.019, respectively for the yield strength, and those for the ultimate strength are 1.592E8 and 8.658, respectively, as shown in Eq. 2 and Eq. 3.

(2)

(3)

where σ_{du} and σ_{su} are the dynamic ultimate strength and the static ultimate strength, respectively. As can be seen from Fig. 16, the fitted curves agree well with the test results. The calibrated equations could be used in dynamic analysis of structures [8,40].

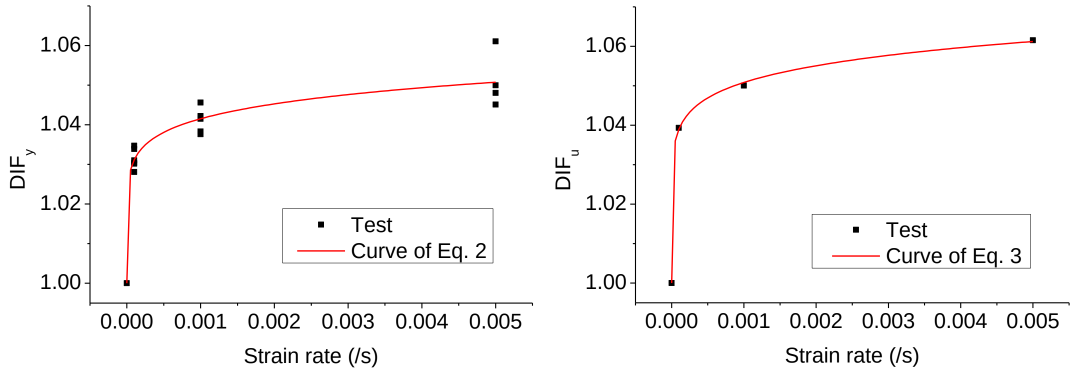

(a) Yield strength (b) Ultimate strength

Fig. 16 Fitting curves of strength enhancement due to strain rate

5. Suggestions on procedures of coupon test of HSS

The current mainstream specifications of coupon test such as Australian Standard (AS) [20], European Code (BSI) [21], American Specification (ASTM) [22], and Chinese Standard [23] allow changes of loading rate in the process of the coupon test for determining the yield strength and ultimate strength. However, the experimental results of the current study show that for HSS Q690 the ultimate strength is as sensitive to the loading rate as the yield strength. As can be seen from Section 4, strain rate significantly affects both the yield strength and ultimate strength. Hence, a constant strain rate is recommended in the whole process of the tensile coupon test. The strain rate of the tensile coupon test is recommended to be in the range from 0.0001 /s to 0.001 /s.

To obtain the static mechanical properties of steel material, tensile coupon test with two displacement-controlled holds is recommended. However, one monotonic tensile test is recommended to be conducted first to obtain the yield strain and ultimate strain of the material. One of the holds is at the strain slightly larger than the yield strain and the other is at the strain slightly smaller than the ultimate strain. For the hold near the yield strain, the pre-strain of 0.01 could be adopted. For the hold near the ultimate strain, the pre-strain is recommended to be 0.01 smaller than the ultimate strain. Table 9 summarizes the main differences between the procedure of coupon test in the current standards and the propose procedure.

The dynamic mechanical properties of steel material at different strain rates could be obtained from monotonic tensile coupon test with different loading rates. For HSS Q690, the dynamic properties could by obtained according to the calibrated C-S in Section 4, alternatively. It should be noted that the range of strain rate in the current experimental study is from 0.0001 /s to 0.005 /s. Hence, the calibrated Eq. (2) and Eq. (3) may not suit the strain rate that is larger than 0.005 /s, for which case monotonic tensile test with the considered strain rate is needed.

Table 9 Comparison between procedure of coupon test in the current standards and the propose procedure

Items	Current standards [20-23]	Proposed method (MPa)
Loading mode	Monotonic tensile test	Tensile test with two displacement-controlled holds
Whether allow change of loading rate during	Yes	No

6. Conclusions

This paper experimentally studied the effect of loading mode on the mechanical properties of HSS Q690, and their application on tensile coupon tests of HSS. Test results obtained from three loading modes, namely monotonic tensile coupon test, tensile coupon test with displacement-controlled holds, and tensile coupon test with strain-controlled holds, were compared to identify the proper loading mode for obtaining static mechanical properties of HSS. Effects of pre-strain, loading rate, and hold times on the stress relaxation during the holds of the coupon test were also investigated. The following key findings were noted:

- The ultimate strength of HSS Q690 is as sensitive to the loading rate as the yield strength. The yield strength, ultimate strength, and the ultimate strain of steel Q690 both increase with the increase of strain rate. The effect of strain rate on the elastic modulus is small for the considered strain rates.
- Stress relaxation has negligible effect on the dynamic ultimate strength and ultimate strain on steel Q690. The largest difference of the ultimate strength induced by loading mode was 6.2 MPa which is less than 1% of the ultimate strength of the material, and the largest difference of the ultimate strain was 5.8E-3.
- The stress drop during the stress relaxation increases with the increase of pre-strain and strain rate. The normalized stress drop at the pre-strain of 0.04 could be 37.4% larger than that at the pre-strain of 0.01. The normalized stress drop of specimen with strain rate of 0.001 /s could be 27.7% larger than that with strain rate of 0.0001 /s. The hold at the strain of 0.01 has little effect on the stress drop of stress relaxation at the pre-strain of 0.04.
- Stress jump occurred after the stress relaxation. The value of stress jump increases with the increase of pre-strain and strain rate. Effect of the pause time on the stress jump was not obvious.
- The static mechanical properties of steel could be obtained from tensile test with two displacement-controlled holds, instead of strain-controlled holds. Suggestions on the procedure of tensile coupon test to obtain both the static and dynamic mechanical properties of HSS were proposed.
- Based on the test results of the coupon tests presented in this paper, the values of parameters of the Cowper-Symonds model were calibrated to consider the effect of strain rate on the dynamic yield strength and ultimate strength, respectively, of HSS Q690. The values of the parameters C and P are 1.203E8 and 8.019, respectively, for the yield strength, and those for the ultimate strength are 1.592E8 and 8.658, respectively.

7. Acknowledgement

This work is supported by the Research Grants Council of the Hong Kong Special Administrative Region, China with Grant No. PolyU 152650/16E, the National Natural Science Foundation of China with Grant No. 51908560, and the Hunan Provincial Science and Technology Department under Grant No. 2017SK1010.

References:

[1] L. Hai, F. Sun, C. Zhao, G. Li, Y. Wang, Experimental cyclic behavior and constitutive modeling of high strength structural steels, Constr Build Mater. 189 (2018) 1264-85.

[2] F. Hu, G. Shi, Constitutive model for full-range cyclic behavior of high strength steels without yield plateau, Constr Build Mater. 162 (2018) 596-607.

[3] S. Lee, B. Uy, S. Kim, Y. Choi, S. Choi, Behavior of high-strength circular concrete-filled steel

tubular (CFST) column under eccentric loading, Constr Build Mater. 67 (2011) 1-13.

[4] Y. Wang, G. Li, S. Chen, F. Sun, Experimental and numerical study on the behavior of axially compressed high strength steel box-columns, Eng Struct. 58 (2014) 79-91.

[5] N. Nguyen, T. Pham, S. Kim, Characterization of strain rate effects on the plastic properties of structural steel using nanoindentation, Constr Build Mater. 163 (2018) 305-14.

[6] E. Cadoni, L. Fenu, D. Forni, Strain rate behaviour in tension of austenitic stainless steel used for reinforcing bars, Constr Build Mater. 35 (2012) 399-407.

[7] B. Jiang, G. Li, B. Izzuddin, Dynamic performance of axially and rotationally restrained steel columns under fire. J Constr Steel Res. 122 (2016) 308-15.

[8] B. Jiang, G. Li, L. Li, B. Izzuddin, Simulations on progressive collapse resistance of steel moment frames under localized fire. J Constr Steel Res. 138 (2017) 380-8.

[9] B. Jiang, M. Wang, Y. Shen, Y. Li, 2020. Robustness assessment of planar steel frames caused by failure of a side column under localized fire, Struct Des Tall Spec. e1711. https://doi.org/10.1002/tal.1711.

[10] T. Li, G. Li, Y. Wang, Residual stress tests of welded Q690 high-strength steel box- and H-sections, J Constr Steel Res. 115 (2015) 283-9.

[11] T. Ma, Y. Hu, X. Liu, G. Li, K. Chung, Experimental investigation into high strength Q690 steel welded H-sections under combined compression and bending, J Constr Steel Res. 138 (2017) 449-62.

[12] L. Huang, G. Li, X. Wang, C. Zhang, L. Choe, M. Engelhardt, High temperature mechanical properties of high strength structural steels Q550, Q690 and Q890, Fire Technol. 54(6) (2018) 1609-28.

[13] W. Wang, K. Wang, V. Kodur, B. Wang, Mechanical properties of high-strength Q690 steel at elevated temperature, J Mater Civil Eng. 30(5) (2018) 4018062.

[14] EN1993- 1- 2. Eurocode 3: Design of steel structures, Part 1- 2: Generalrules - structur al fire design, European Committee for Standardization, Brussels, 2005.

[15] CECS 200：2006. Technical code for fire safety of steel structure in buildings, China Association for Engineering Construction Standardization, Beijing, China, 2006 (in Chinese).

[16] G. Li, H. Lyu, C. Zhang, Post-fire mechanical properties of high strength Q690 structural steel, J Constr Steel Res. 132 (2017) 108-16.

[17] L. Kang, M. Suzuki, H. Ge, B. Wu, Experiment of ductile fracture performances of HSSS Q690 after a fire, J Constr Steel Res. 146 (2018) 109-21.

[18] S. Chen, S. Jiang, H. Guo, H. Cao, Y. Luo, K. Lan, Mechanical and ductile fracture performances of high strength structural steel Q690 after a fire: experimental investigation, Procedia Eng. 210 (2017) 496-503.

[19] F. Wang, E. Lui, Experimental study of the post-fire mechanical properties of Q690 high strength steel, J Constr Steel Res. 167 (2020) 105966.

[20] AS 1391-2007. Metallic materials — tensile testing at ambient temperature, Standards Association of Australia, Sydney, Australia, 2007.

[21] BS EN ISO 6892-1:2006. Metallic materials — Tensile testing Part 1: Method of test at room temperature, British Standards Institution, London, UK, 2016.

[22] E8/E8M-16a. Standard Test Methods for Tension Testing of Metallic Materials, American Association State, USA, 2016.

[23] GB/T 228.1-2010. Metallic materials — Tensile testing— Part 1: Method of test at room temperature. Standardization Administration of China, Beijing, China, 2010.

[24] Y. Huang, B. Young, The art of coupon tests, J Constr Steel Res. 96 (2014) 159-75.

[25] P. Haupt, A. Lion, Experimental identification and mathematical modeling of viscoplastic material behavior, Mechanics and Thermodynamics. 7 (1995) 73-96.

[26] G. Cowper, P. Symonds, Strain-hardening and strain-rate effects in the impact loading of cantilever beams, Brown University, 1957.

[27] E. Krempl, F. Khan, Rate (time)-dependent deformation behavior: an overview of some properties of metals and solid polymers, Int J Plasticity. 19(7) (2003) 1069-95.

[28] K. Hariharan, P. Dubey, J. Jain, Time dependent ductility improvement of stainless steel SS 316 using stress relaxation, Mat Sci Eng A-Struct. 673 (2016) 250-6.

[29] M. Mohebbi, A. Akbarzadeh, Y. Yoon, S. Kim, Stress relaxation and flow behavior of ultrafine grained AA 1050, Mech Mater. 89 (2015) 23-34.

[30] A. Seeger, J. Diehl, S. Mader, H. Rebstock, Work-hardening and work-softening of face-centred cubic metal crystals, Philos Mag. 2(15) (1957) 323-50.

[31] E. Hart, H. Solomon, Load relaxation studies of polycrystalline high purity aluminium, Acta Metall. 21 (1973) 295-307.

[32] W. Quach, B. Young, Material properties of cold-formed and hot-finished elliptical hollow sections, Adv Struct Eng. 18(7) (2015) 1101-14.

[33] N. Saliba, L. Gardner, Cross-section stability of lean duplex stainless steel welded I-sections, J Constr Steel Res. 80 (2013) 1-14.

[34] A. Varma, A. Gokhale, J. Jain, K. Hariharan, P. Cizek, M. Barnett, Investigation of stress relaxation mechanisms for ductility improvement in SS316L, Philos Mag. 98(3) (2018) 165-81.

[35] I. Eipert, G. Sivaswamy, R. Bhattacharya, M. Amir, P. Blackwell, Improvement in ductility in commercially pure titanium alloys by stress relaxation at room temperature, Key Eng Mat. 611 (2014) 92-8.

[36] S. Hannula, M. Korhonen, C. Li, Strain aging and load relaxation behavior of type 316 stainless steel at room temperature, Metall Mater Trans A. 17A (1986) 1757-67.

[37] K. Hariharan, O. Majidi, C. Kim, M. Lee, F. Barlat, Stress relaxation and its effect on tensile deformation of steels, Mater Design. 52 (2013) 284-8.

[38] Y. Xu, S. Zhang, M. Cheng, H. Song, S. Wang, Effect of loading modes on mechanical property and strain induced martensite transformation of austenitic stainless steels, Acta Metall Sin. 49(7) (2013) 775-82.

[39] X. Li, J. Li, W. Ding, S. Zhao, J. Chen, Stress relaxation in tensile deformation of 304 stainless steel, J Mater Eng Perform. 26(2) (2017) 630-5.

[40] A. Shishegaran, M.R. Khalili, B. Karami, T. Rabczuk, A. Shishegaran, Computational predictions for estimating the maximum deflection of reinforced concrete panels subjected to the blast load. Int J Impact Eng. 139(2020) 103527.